1.2 FRACTURE TESTING AND EVALUATION PROCEDURES FOR MINIATURE F82H DCT SPECIMENS – T. S. Byun (Oak Ridge National Laboratory) and D. Hamaguchi (Japan Atomic Energy Agency)

OBJECTIVE

Fracture testing and evaluation of highly radioactive fusion reactor materials require miniaturized specimens and simplified test techniques. The goal of this work is to establish a new fracture testing and evaluation procedure for highly radioactive F82H disk compact tension (DCT) specimens.

SUMMARY

Fracture toughness testing in high radiation areas using miniaturized specimens has become a major challenge in the evaluation of highly radioactive materials as it requires high precision recording of load-displacement data, including loading-unloading cycles, often in vacuum or controlled environments. A new testing and analysis procedure was established to test small disk compact tension (DCT) fracture specimens irradiated to high doses. This report summarizes the major components of the new procedure: a simplified testing technique to obtain minimum datasets needed for analysis and a simplified normalization method for evaluating crack resistance (J-R) data. In application, two sets of fracture test data obtained from 4.72 and 3.56 mm thick DCT specimens of nonirradiated low-activation ferritic-martensitic steels (F82H steels) were analyzed and the results are discussed focusing on the effect of side grooves and on the recommendation for data validity.

PROGRESS AND STATUS

Introduction

The structural materials for fusion reactors require excellent performance at high temperatures and high doses as the reactor designs aim at increasingly higher thermal efficiency and longer lifetime. Materials evaluation procedures need to handle very high dose (>10 dpa) specimens that can limit specimen size for reasonable cost and efficiency of work in radiation area. Compared to the evaluation of current pressurized water reactor (PWR) materials, therefore, more extreme miniaturization techniques are required for the property evaluation of high dose materials. More restricted testing conditions such as high temperature and environmental control can further aggravate the difficulties in the evaluation procedure in high radiation areas. For the fracture testing in a high temperature vacuum furnace, for instance, instrumentation for displacement measurement from a miniature fracture specimen is extremely difficult and thus needs to be minimized. This research aimed to establish miniaturized fracture testing and evaluation techniques that can remove some of the experimental difficulties in high radiation area.

A simplified procedure for static fracture testing and dada analysis was established to test miniature disk-compact tension (DCT) specimens irradiated to high doses. The standard fracture testing procedure needs a high precision recording on loading-unloading cycles. In reality, however, we often experience that the measurements of unloading compliance from miniature specimens become highly inaccurate at elevated or high temperature because of significant friction and plastic deformation at contact surfaces. Therefore, the major change made in the testing procedure is removing the attachment of external (clip-on) gage. In data analysis the issues caused by this change were resolved by adopting the curve normalization method for J-R curve construction and by modifying other detailed calculation steps accordingly. This report summarizes the major components of the new procedure.

In addition, to demonstrate the applicability of the new procedure, the new procedure has been applied to the baseline tests for nonirradiated low-activation ferritic-martensitic steels (F82H steels). Two sets of fracture test data obtained, respectively, from the 4.72 and 3.56 mm thick DCT specimens of were analyzed and the results are discussed. Application results demonstrated that the newly established

procedure can produce nearly identical J-R curve as the traditional unloading compliance method. It was also shown that the miniature DCT specimens without side grooves can induce significant variation or overestimation in the fracture toughness of the test material.

Experimental and Analysis Procedures

Simplification of data acquisition for fracture test in high radiation area

In the post-irradiation fracture tests using remote manipulator in hotcells, any data acquisition through direct connections to specimens can cause major drawbacks in addition to the general difficulties in handling miniature specimens. Use of some sensing devices becomes prohibitively difficult in the miniature specimen tests in a controlled environment. It should be therefore considered if the test technique that uses gage lead or electrode directly attached to the specimen can be avoided. Since the normalization method requires the simplest datasets to obtain a J-R curve, i.e., the load-displacement curve and optical measurements of initial and final crack lengths, it was chosen for the fracture testing of miniature DCT specimens. Further, simplification in data acquisition has been pursued based on the consideration that the measurement of highly accurate displacement may not be needed as explained below.

In typical fracture test systems, a precision displacement gage, such as Wheatstone bridge type clip gage or linear variable differential transducer (LVDT), is usually attached to the fracture specimen to measure the specimen-mouth displacement in compact tension specimens or the axial displacement (deflection) in bend-bar type specimens. In actual J-R curve calculation (*ASTM Standard Test Method E1820)*, the J-integral is divided into two components of elastic and plastic works. The elastic J component is a well-defined function of load, crack length, and elastic constants, none of which requires displacement measurement. The plastic J component indeed requires displacement data but plastic component only. These detailed practices in J-evaluation indicate that the elastic component of measured displacement is not used in any methods of J-R curve calculation except for compliance data in the unloading compliance method. In the normalized curve method, in particular, the plastic displacement at each point can be easily separated from total displacement using the initial slope of load-displacement curve and updated compliance value, which is calculated by a function of crack length.

In a displacement control mode, most mechanical testing systems are controlled by the displacement reading from built-in devices: an LVDT is usually embedded in the actuator of a servohydraulic test system, and the rotation encoding signal is converted to the crosshead movement or displacement in motor-driven systems. These displacement data obtained from the built-in devices include the displacement components of all parts and contacts in the entire load train, and therefore, are usually not accurate enough to be used in the unloading compliance method, where an accurate measurement of elastic unloading slopes is essential for converting those to crack length data. In the normalization method, however, any non-plastic components of total displacement can be easily removed in the J-R curve calculation procedure: the displacement reading from a built-in device can be used to extract the necessary plastic component of displacement. In this work, therefore, a major simplification was made in the testing setup: attachment of additional gage such as clip gage was eliminated. The following sections describe the normalization method modified for the simple data acquisition along with application examples of F82H ferritic-martensitic steel specimens.

Materials and specimens

The test material used for this development is the Japanese low-activation ferritic-martensitic (LAFM) steel H82H with a nominal composition of Fe-8Cr-2W-0.2V-0.04Ta-0.1C (in wt.%). The steel was in normalized (at 1040°C for 40 min) and tempered (at 1040°C for 1 h) condition. As listed in Table 1, two sizes of miniature DCT specimens were tested: four 3.56 mm thick DCTs and five 4.72 mm thick DCTs. The smaller DCT specimens do not have size grooves but one specimen, while the larger specimens have a 10% side groove at each side. The flow stress (the average of YS & UTS) and the Young's

modulus (*E*) used for calculations were typical values measured for the material. Also, the initial and final crack lengths, a_0 and a_f, were measured from the boundaries of the surfaces from precracking, stable crack growth on J-R testing, and post-test fracture. The initial crack length is determined by the average of nine point measurements on the front line of precracking growth. The final crack lengths were measured in the same manner, but either heat tinting or fatigue cracking was applied to the as-tested specimens before final separation for making the stable and final fracture surfaces discernible.

Table 1. Dimensions and basic properties of DCT specimens

Specimen I.D.	S_Y [MPa]	*B* [mm]	*Bn* [mm]	*Be* [mm]	*W* [mm]	*E* [GPa]	a_0 [mm]	a_f [mm]	*Dia.* [mm]
F82H 0.14DCT-22C-A	586	3.56	3.56*	3.56	8.13	206.8	3.31	5.21	9.6
F82H 0.14DCT-22C-B	586	3.56	3.56*	3.56	8.13	206.8	3.80	5.50	9.6
F82H 0.14DCT-22C-C	586	3.56	3.56*	3.56	8.13	208	3.65	4.90	9.6
F82H 0.14DCT-22C-D	586	3.56	2.63**	3.32	8.13	208	4.25	5.10	9.6
F82H 0.18DCT-22C-A	586	4.72	3.78	4.54	9.25	206.8	4.58	6.05	12.5
F82H 0.18DCT-22C-B	586	4.72	3.78	4.54	9.25	206.8	4.55	6.27	12.5
F82H 0.18DCT-22C-C	586	4.72	3.78	4.54	9.25	206.8	4.93	6.55	12.5
F82H 0.18DCT-22C-D	586	4.72	3.78	4.54	9.25	206.8	4.92	6.55	12.5
F82H 0.18DCT-22C-E	586	4.72	3.78	4.54	9.27	208	4.65	5.87	12.5

Note A: S_Y = flow stress, B, Bn, Be = gross, net, and effective thickness, W = width of specimen
*Note B: *no side groove, **13% side groove at each side; all 0.18 DCTs have 10% side grooves.*

<u>The modified curve normalization method</u>

The descriptions given below follow those of the standard test method ASTM E1820. Only exception is the process to use the displacement data either from a built-in device or from cross-head movement. The same equations and definitions as in the standard are used below for being easily recognized by readers.

Record load-displacement data: The first step of the procedure is to produce load-displacement curve (P_i – v_i dataset). In this work the load-displacement data were recorded with or without attachment of clip gage. Each static fracture test was performed at a displacement rate of about 0.5 mm/min at room temperature until the load decreases to about 50% of the maximum load. Figure 1 displays an example for the load-displacement curve obtained from a 4.7 mm thick F82H DCT specimen.

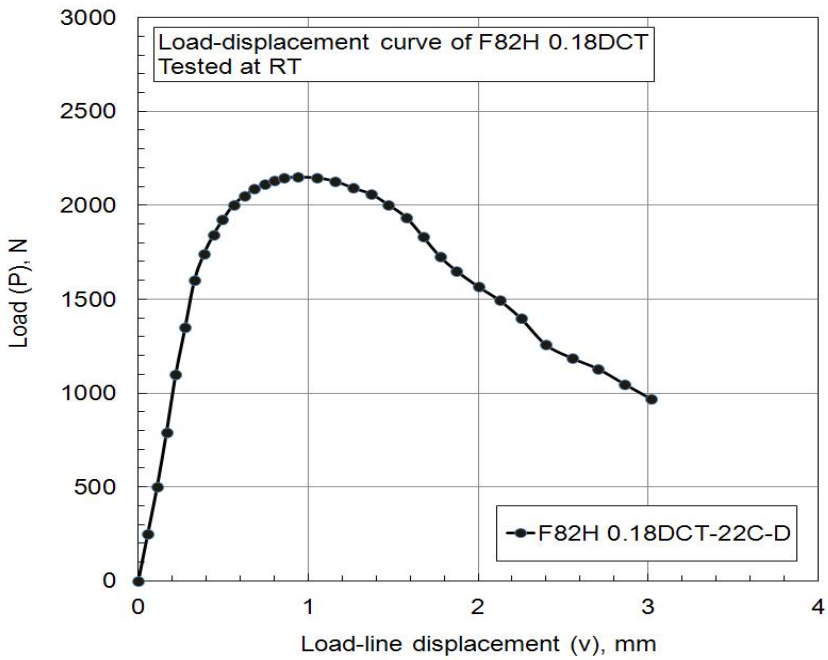

Figure 1. A load-displacement curves for a 4.7 mm thick DCT specimen. The displacement was recorded using a clip gage and this curve is after removing the loading-unloading lines.

Calculation of J-integral: Although different techniques are used for evaluation of crack length, common equations are used for calculation of *J*-integral and stress intensity factor *K* (ASTM E1820). Those equations are summarized first as below since many of them are intermingled in the application of normalized curve method. The total J-integral at point (i) is defined as the sum of elastic and plastic components ($J_{e(i)}$ and $J_{p(i)}$):

$$J_{(i)} = J_{e(i)} + J_{p(i)} = \frac{K_{(i)}^2(1-\nu^2)}{E} + J_{p(i)} \quad (1)$$

where *E* is the elastic modulus, *v* the Poisson ratio (=0.28), and K the stress intensity factor or linear-elastic component of fracture toughness. When all load-displacement and geometrical parameters are known, the plastic component J_p can be calculated by

$$J_{p(i)} = \frac{\eta A_p}{B_N b} \quad (2)$$

where the A_p is the plastic energy applied to the specimens or area below load-plastic displacement curve, Δa crack length dependent dimensional parameter, B_N the net specimen thickness, and *b* the uncracked ligament (=*W*-*a*; *W* is the specimen width). In practical calculations, however, a discretized equation is used:

$$J_{p(i)} = \left[J_{p(i-1)} + \left(\frac{\eta_{(i-1)}}{b_{(i-1)}}\right)\frac{A_{p(i)}-A_{p(i-1)}}{B_N}\right]\left[1-\gamma_{(i-1)}\frac{a_{(i)}-a_{(i-1)}}{b_{(i-1)}}\right] \quad (3)$$

where $a_{(i)}$ and $b_{(i)}$ are the crack length and uncracked ligament at point (i), respectively. Note that in this article all parameters at point (i) and (i-1) are defined in the same manner. Also, the η and γ parameters, and plastic energy increment are defined as below:

$$\eta_{(i-1)} = 2.0 + 0.522b_{(i-1)}/W \quad (4)$$

$$\gamma_{(i-1)} = 1.0 + 0.76b_{(i-1)}/W \quad (5)$$

$$A_{p(i)} - A_{p(i-1)} = \frac{[P_{(i)}+P_{(i-1)}][v_{p(i)}-v_{p(i-1)}]}{2} \quad (6)$$

The stress intensity factor $K_{(i)}$ is given as a function of load P and geometrical parameters only:

$$K_{(i)} = \frac{P_{(i)}}{(EB_N W)^{1/2}} \frac{\left[(2 + a_{(i)}/W)(0.76 + 4.8(a_{(i)}/W) - 11.58(a_{(i)}/W)^2 + 11.43(a_{(i)}/W)^3 - 4.08(a_{(i)}/W)^4\right]}{(1 - a_{(i)}/W)^{3/2}} \quad (6)$$

Calculation of normalized P-v curve up to the maximum load point: This section of a load-displacement curve corresponds to the crack blunting regime or the initial section of a J-R curve with a steep slope of $2\sigma_Y$. As described in the standard test method, the normalized load and displacement ($P_{N(i)}$, $v'_{p(i)}$) are defined as generalized parameters that are insensitive to the geometry of test specimen and given in stress and strain units, respectively. The normalized load and displacement up to, but not including the maximum load is calculated by:

$$P_{N(i)} = \frac{P_{(i)}}{\mathrm{WB}\left[\frac{W-a_{(i)}}{W}\right]^{\eta(i)}} \quad (7)$$

$$v'_{p(i)} = \frac{v_{p(i)}}{\mathrm{W}} = \frac{v_{(i)} - C_{(i)}P_{(i)}}{\mathrm{W}} \quad (8)$$

Here, the crack length $a_{(i)}$ and compliance $C_{(i)}$ (=$C_{LL(i)}$ if measured with load-line displacement) calculated by:

$$a_{(i)} = a_0 + \frac{J_{(i)}}{2\sigma_Y} \quad (9)$$

$$C_{LL(i)} = \frac{1}{EB_e}\left(\frac{1+a_{(i)}/W}{1-a_{(i)}/W}\right)^2 \left[2.0462 + 9.6496\left(\frac{a_{(i)}}{W}\right) - 13.7346\left(\frac{a_{(i)}}{W}\right)^2 + 6.1748\left(\frac{a_{(i)}}{W}\right)^3\right] \quad (10)$$

As can be quickly realized in practical calculation, the evaluation of these equations requires to solve circular references among parameters: in the above four equations, for example, the $a_{(i)}$ needs to be evaluated first to calculate others such as $\eta_{(i)}$, $J_{(i)}$, $C_{LL(i)}$, and then $P_{N(i)}$. Therefore, we need to adopt an iteration technique or a simpler technique of using previously calculated values for the (i-1)th point. In this work, the latter technique is used as data acquisition interval can be easily adjusted to be very small so that the error from using the values of the (i-1)th point instead of those of the (i)th point becomes negligible.

Calculation of normalized load and displacement from the max-load point to final point: A major modeling is needed in this step, representing the major crack growth to final failure, as the crack blunting line (eq. 9) cannot be used. The accuracy of the model depends on how we connect the maximum load point with the final point (known from the measurement of final crack length) in the normalized load-displacement curve ($P_{N(i)}$-$v'_{p(i)}$ curve).

A line should be drawn from the final normalized load-displacement pair tangent to the curve around the maximum load point calculated in the previous step. The connection with a simple linear line can provide highly accurate outcome for J-R curve in most cases although use of a normalization function with four

fitting coefficients is recommended in the standard method. A simpler but non-linear four parameter function was suggested by the author and has been used for high strength steels:

$$P_{N(i)} = \frac{P_{N(m)} + x\left[v'_{p(i)} - v'_{p(m)}\right]}{1 + y\left[v'_{p(i)} - v'_{p(m)}\right]^2} \qquad (11)$$

where the point denoted by the subscript '*m*' is the maximum load point, and the variables *x* and *y* are changed until the best fit curve is reached. Among the four parameters to be determined the x and y are true variables while the other two are determined at the maximum load (m) point.

Two criteria used for searching the best fitting function are (a) if the functional continuity between the fitting function and the calculated data using the blunting line ($J=2\Delta_Y\Delta a$) is achieved around the maximum load point and (b) if the normalized load by the fitting function matches the value calculated from the measured final crack length. An example displayed for a normalized load versus displacement curve for the 4.7 mm thick DCT specimen is provided in Figure 2, which corresponds to the non-normalized curve given in Figure 1.

Calculation of crack lengths from the max-load point to final point: As the full normalized load versus displacement is established, the crack extension beyond the crack blunting regime can be easily calculated by an inverse function of equation (7):

$$a_{(i)} = W\left\{1 - \left[\left(\frac{P_{(i)}}{P_{N(i)}}\right)\left(\frac{1}{WB}\right)\right]^{1/\eta_{(i)}}\right\} \qquad (12)$$

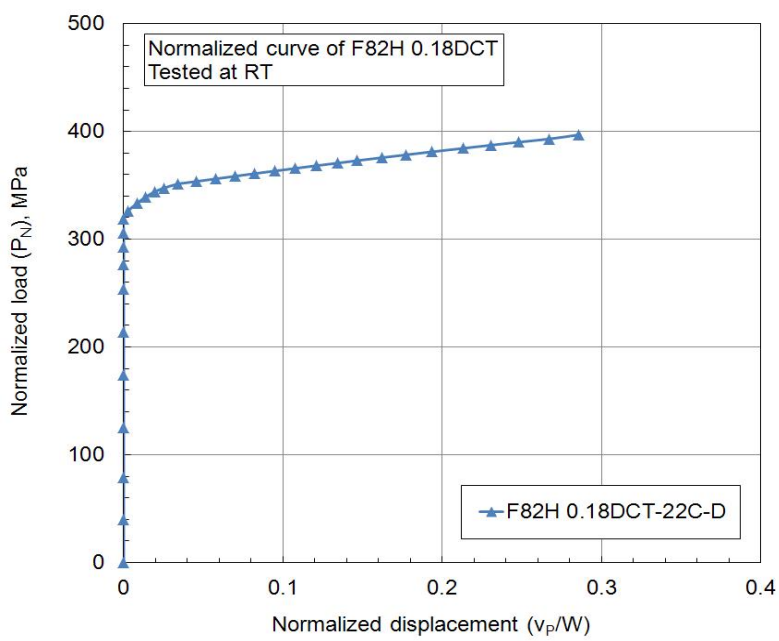

Figure 2. A normalized load versus displacement curve for a 4.7 mm thick DCT specimen

Construction of J-R curve: In the process of calculating crack lengths using normalization, the *J-R* curve, i.e., *J-Δa* curve is simultaneously obtained at each data point since the crack extension amount *Δa* is simply given by $a_{(i)} - a_0$. The J-R curve obtained for the present example case is displayed in Fig. 4. The

comparison with the curve from the standard unloading complication method indicates that the J-integral values from the two methods agree well.

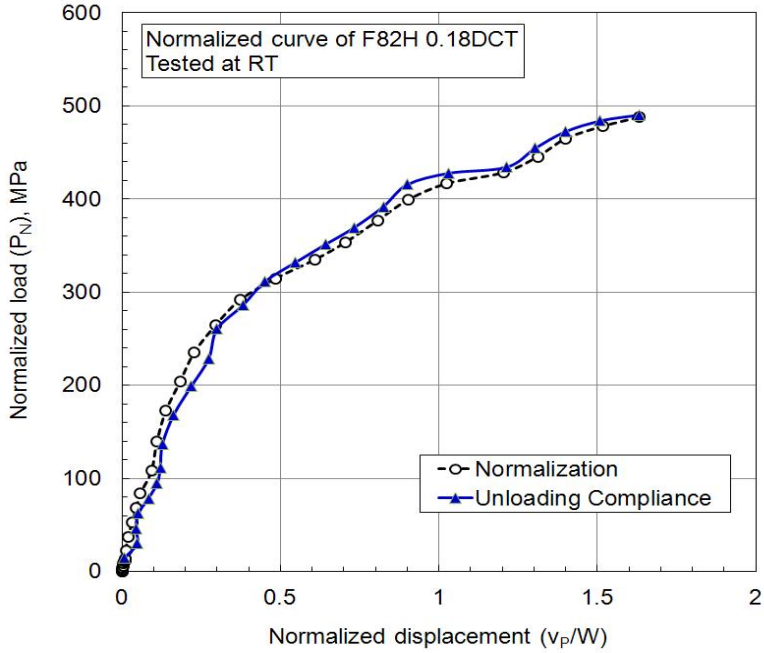

Figure 3. An example of J-R curve obtained by the normalization method. It is compared to the curve from the standard unloading compliance method (for specimen F82H 0.18DCT-22C-D).

Results and discussion

Load line-displacement and J-R curves

Figures 5 and 6 display the load versus displacement curves for the DCT specimens. It should be noted that the curves for the first two cases, F82H-0.18DCT-22C-A and –B, were recorded with clip-on gage, while the other curves without the gage. Significantly different load-displacement traces were recorded from the DCT specimens primarily due to the differences in initial crack length and net thickness. Further, the smaller DCT specimens without side grooves (A & B) also incurred larger plasticity zone.

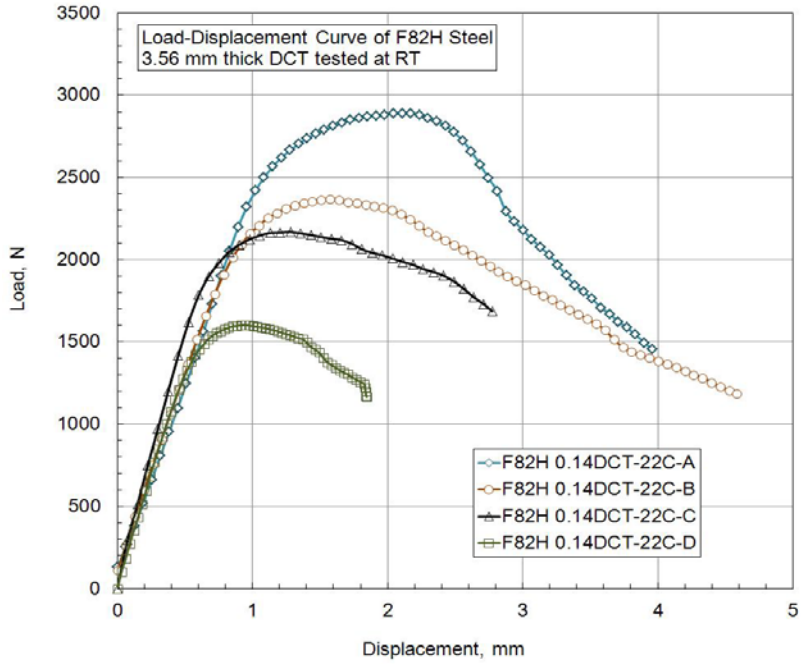

Figure 4. Load-displacement curves for 3.56 mm thick DCT specimens. Note that no clip-on gage was used: the displacement data were obtained from cross-head movement. No side groove was machined to the three specimens F82H 0.14DCT-22C-A to C but had side 13% grooves in the D specimen.

Figures 7 and 8 present the J-R curves constructed from the specimen geometry data (Table 1) and the load-displacement curves (Figs. 6 and 7) using the simplified curve normalization method described in Section 2. The J-R curves from the first two smaller DCTs (F82H 0.14DCT-22C-A&B) show slightly different behaviors. The J-integral value of the specimen A increased to higher values in low crack extension (Δa) range but it went lower than the curve for specimen B from Δa = ~0.7 mm. As a result, the specimen A displayed lower slope or tearing modulus. Since these smaller specimens did not have side grooves, the development of plasticity zone should be less uniform between the specimens when compared to the side grooved specimens. It is believed that the differences in plastic zone size and initial crack length have caused such different J-R behaviors in the 3.6 mm thick DCT specimens.

In Figure 6, the other smaller DCT specimens (F82H 0.14DCT-22C-C&D) showed similar J-R curves although they were tested with and without side grooves (see Table 2). Compared to the specimen C, the specimen D showed lower load-displacement curve due to larger initial crack length and side grooves; however, both J-R traces are similar for both specimens. In general, the specimen with a larger initial crack length results in a steeper increase, especially in J value in the later part of J-R curve. It is interesting, however, to observe that the slope in the later part of J-R curve in D is not higher than that of the specimen C. This is believed to be because of the constrained development of plastic zone in the specimen D with side grooves. It is also very evident that these specimens (F82H 0.14DCT-22C-C&D) have much lower J-R curves than the other two specimens (F82H 0.14DCT-22C-A&B). The difference is too large to explain with specimen geometry reasons; a metallurgical difference is expected to be found between these seemingly two different materials.

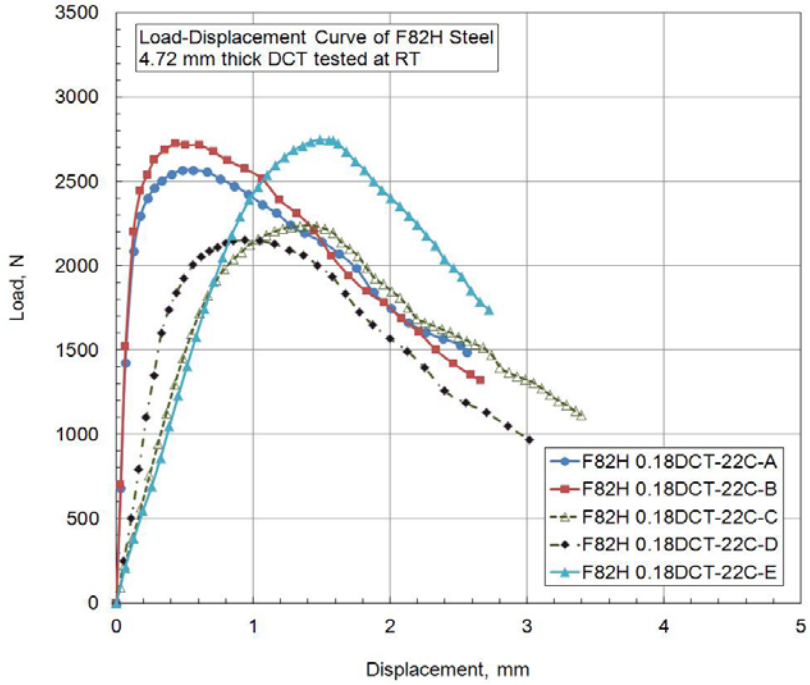

Figure 5. Load-displacement curves for 4.72 mm thick DCT specimens. Note (1) that the curves for the first two cases, F82H-0.18DCT-22C-A and B, were recorded with clip-on gage, while the other curves without the gage and (2) that all the 0.18DCT specimens have a nominal thickness of 0.18 inch (~4.7 mm) and 10% side groove at each side.

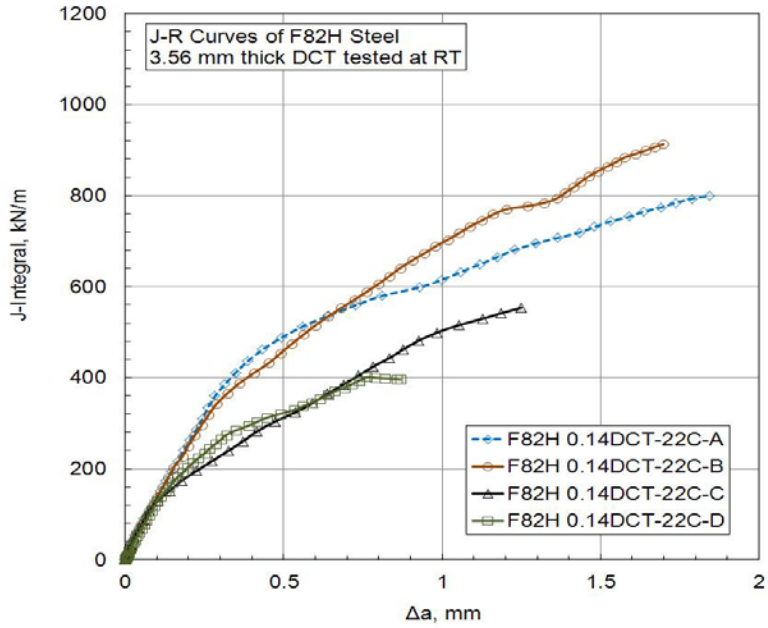

Figure 6. J-R curves generated for F82H 0.14DCT specimens.

For the 4.7 mm thick DCTs with side grooves, Figure 7 confirms that the different load-displacement curves result in similar J-R curves. This might be because the side grooves have caused more orderly crack extension and thus smaller plastic zones developed in these specimens are relative uniform. This result also confirms that the J-evaluation process using pure plastic displacement only has been correctly developed.

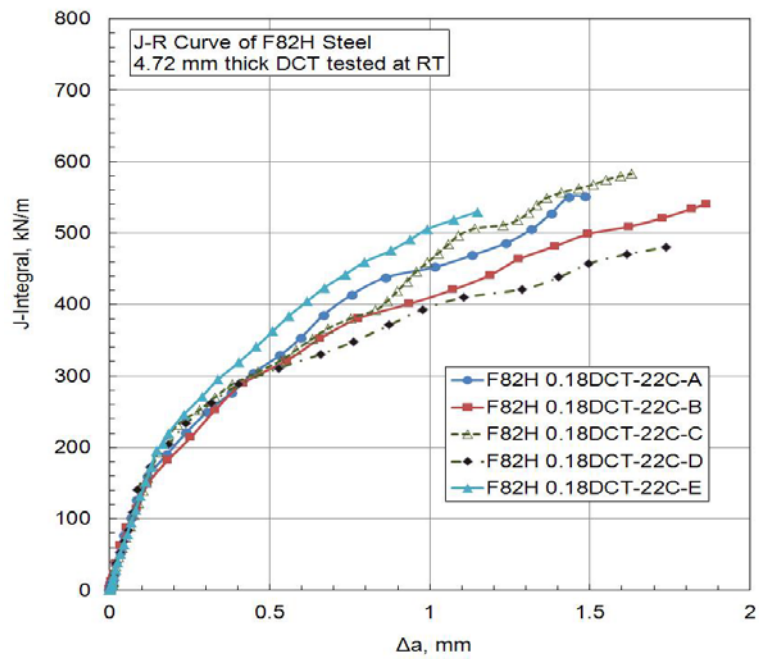

Figure 7. J-R curves generated for F82H 0.18DCT specimens.

The final step of fracture evaluation procedure is to determine fracture toughness values. Following the ASTM standard method E1820, the interim fracture toughness values (J_Q) were determined at the intersection of the constructed J-R curves and the 0.2 mm offset line of the blunting line ($=2\sigma_Y\Delta a$). The final fracture toughness data are also given in the form of stress intensity factor, K_{JQ}, which can be converted from the J_Q data using the following relationship:

$$K_{JQ} = \sqrt{(J_Q \cdot E)/(1-\nu^2)}, \qquad (13)$$

The results of this toughness determination process are summarized in Table 2. Comparing the values in Table 2, the side grooved 4.7 mm thick specimens have yielded relatively uniform fracture toughness values. The maximum difference among K_{JQ} values was only 19 MPa√m, which is about 7% of the fracture toughness values listed.

The last column lists the slope *dJ/da* for reference. These values can be easily converted to the tearing modulus *dJ/(Eda*). Further, it is worth knowing that the fracture toughness values corresponding to the intersection of J-R curve with a 0.1 mm shifted line can be approximately calculated form the fracture toughness data provided in Table 2 using these slope data.

It is worth noting that the fracture toughness parameters in Table 2 are still in 'interim' status as the validity check is not performed for the data. The toughness values for the specimens without side grooves, in particular, are expected to be invalid mainly because of the curved crack front line and overly higher plasticity. It is advised to use these data for comparison purposes only and a scaling process using a size effect model is needed prior to use in engineering analyses.

Table 2. Fracture toughness parameters

Specimen	*J_O [N/mm or kJ/m^2]	K_{JO} [MPa√m]	dJ/da [GPa]
F82H 0.14DCT-22C-A	513	341	275
F82H 0.14DCT-22C-B	495	335	503
F82H 0.14DCT-22C-C	282	253	389
F82H 0.14DCT-22C-D	312	266	238
F82H 0.18DCT-22C-A	277	251	365
F82H 0.18DCT-22C-B	253	240	308
F82H 0.18DCT-22C-C	297	260	273
F82H 0.18DCT-22C-D	288	256	210
F82H 0.18DCT-22C-E	319	269	409

*Determined at the intersection between 0.2 mm offset blunting line and J-R curve ($J_Q = J_{0.2mm}$)

CONCLUSIONS

A modified procedure for fracture testing and J-R curve construction has been developed to test miniature disk compact tension (DCT) specimens in high radiation areas. Fracture testing procedure was simplified by eliminating any externally-attached displacement gage. In the J-integral evaluation procedure, the load-displacement curve normalization method for calculation of crack lengths was modified to accommodate the experimental simplification.

The application to the H82H ferritic-martensitic steel DCT specimens confirmed that the newly established procedure can produce nearly identical J-R curve as the traditional unloading compliance method. With the side grooved DCT specimens, where the crack extension and development of plastic zone are strongly guided, highly close J-R curves could be obtained for the DCT specimens with different initial crack sizes.

The application results also indicated that the miniature DCT specimens without side grooves can induce significant variation or overestimation in the fracture toughness of the test material. Introducing side groves is highly recommended in using miniature fracture specimens.

Acknowledgements

This research was sponsored by U.S. Department of Energy, Offices of Fusion Energy Sciences and Nuclear Energy, under Contract DE-AC05-00OR22725 with UT-Battelle, LLC.